INSPECTION OF LASER WELDS WITH ARRAY EDDY CURRENT TECHNIQUE

E. Todorov[1], B. Nagy[1], S. Levesque[1], N. Ames[2], and J. Na[1]

[1]EWI, Technical Division, Columbus, OH 43221
[2]Joe Knows Energy, Columbus, OH 43212

ABSTRACT. Three groups of laser weld specimens made of steel 316L for nuclear applications were fabricated - acceptable, missed seam (MS) and lack of penetration (LOP). An array eddy current technique was developed and investigated. The specimens top and bottom surfaces were scanned parallel and transverse to the weld line. The MS and LOP were easily imaged, detected and sized. Additional flaw indications were found in visually acceptable weld areas. Limited weld destructive testing was performed validating characteristic eddy current flaw indications.

Keywords: Nondestructive Testing**,** Eddy Current Testing, Advanced Eddy Current Techniques, Eddy Current Array Sensor, Eddy Current Weld Testing, Laser Welding, Nuclear Fabrication.
PACS: 81.70.Ex, 81.20.Vj

INTRODUCTION

There are three major areas where nondestructive evaluation (NDE) techniques are implemented for inspection of nuclear components – fabrication, pre-service, and in-service. One of the main joining processes during nuclear component fabrication is welding. The type of flaw and conditions that must be reliably detected will depend on the welding process, material, geometry, and in particular the component criticality in terms of safety and component failure impact.

Some of the lessons learned from the current reactors in use indicated that the introduction and qualification of better joining processes along with the use of better NDE techniques and automation for data acquisition during fabrication would improve the NDE reliability and reduce the inspection frequency later in-service [1, 2]. The automation of NDE processes can significantly increase the inspection speed, reduce operator fatigue, replace the operator at dangerous environments such as nuclear facilities and reduce the inspection cost. However, the initial cost of technique development and personnel training might be significant.

Electromagnetic and eddy current techniques were found suitable for further development and automation following the analysis of the nuclear industry needs and

current status of the NDE technologies. The conventional eddy current techniques are capable of detecting longitudinal and transverse surface cracks, lack of fusion (LOF), crater cracks, pores, and other surface breaking discontinuities. The disadvantage of surface eddy current techniques is the strong effect of weld crown roughness and irregularities. If the crown is machined flush with the parent metal, the roughness effect is significantly reduced or eliminated, however, the flaw surface opening might be smeared affecting negatively the detectability.

Advanced automated eddy current techniques with single and array sensors have proven very effective for detection, imaging, and quantification of discontinuities and surface treatments [3-7]. For example, reliable detection and sizing of very tight fatigue cracks in weld toe area with the weld crown in place and with the crown machined flush was realized in a study investigating advanced eddy current techniques for weld inspection [3]. The array sensors will allow simultaneous scanning of entire weld surface at several frequencies for detection and sizing of surface and slightly subsurface flaws. Variations of material properties such as inadequate heat treatment, metallurgical phase transformation, and others might also be possible to detect and quantify. The array sensors can be used for either scanning the inspection area or permanently mounted for condition and health monitoring.

One of the objectives of this study was to optimize and demonstrate an automated eddy current array technique for inspection of stainless steel laser weld joints critical to the sustainability and advancement of nuclear fabrication, new reactor design and nuclear power technology.

LASER WELDING PROCESS AND EXPERIMENTAL SPECIMENS

Over the past few decades, major technological advancements in the arena of both high- and low-power lasers have brought laser processing to the forefront of many manufacturing industries (automotive, aerospace, medical, and heavy manufacturing to name a few). The nuclear industry has been using laser welding on fuel assemblies for years, but the lack of large-scale construction projects has somewhat prevented the U.S. commercial nuclear power industry from exploring other applications for laser welding.

Laser welding encompasses a wide variety of processes that offer several potential benefits over traditional arc welding approaches (less distortion, deeper penetration, faster travel speeds to name a few). Autogenous laser welding is preferred when exceptional part fit-up can be obtained and no alloying or filler is needed. High power levels (>30-kW) are capable of single-pass weld penetration exceeding 25-mm, which is far beyond the capabilities of traditional arc-welding techniques. If alloying is required or slight variations in part fit-up are encountered, hybrid laser-arc welding (HLAW) may be more applicable. The HLAW process combines laser welding with gas metal arc welding (GMAW) in the same molten weld pool.

While there has been widespread deployment of laser welding in a number of industries, there has been no concerted focus to date on developing an understanding of material properties and weld quality as they relate to the needs of the nuclear industry. Weld porosity and lack-of-fusion (due to misaligned welds or inadequate penetration) are two examples of discontinuities that could result from the laser welding process.

To assist with the development of NDE techniques for evaluating the weld quality of thick-section laser welds, three groups with total of six laser welds were produced on 316L stainless steel:

- Group 1 – Good (G) quality, full-penetration welds on the weld seam - W1G (HLAW) and W6G (autogenous)
- Group 2 – Partial or lack of penetration (LOP) welds on the weld seam - W8LOP and W9LOP (both autogenous)
- Group 3 – Full-penetration welds with portions missing the weld seam (MS) – W10MS and W11AMS (both autogenous). (NOTE: The attempt to produce a second specimen with missed seam was unsuccessful hence the abbreviation "attempted missed seam" (AMS) for the specimen W11AMS - confirmed by visual and eddy current inspections)

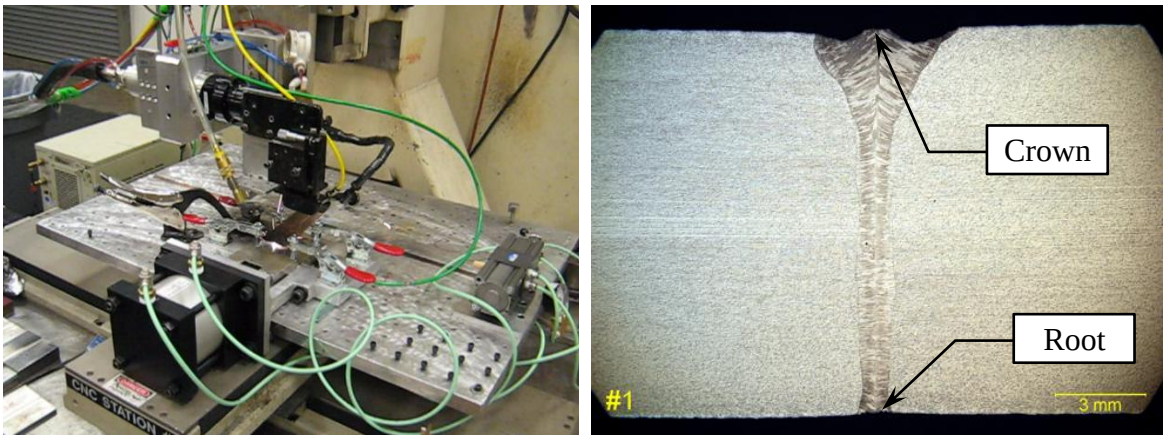

FIGURE 1. Equipment set-up (left) and cross-section of a full-penetration, acceptable hybrid weld (right).

The dimensions of each specimen with weld at the middle were 150- x 150- x 12.5-mm. A 15-kW Fiber Laser was used to produce the single-pass welds on square-butt joints. For the autogenous laser welds, argon shielding gas was used to protect the molten weld pool from atmospheric contaminants. The hybrid laser weld was shielded with a 92% Argon, 8% CO2 mixture. The first group (G) of laser welds targeted high-quality, full-penetration welds. The welds required 12-kW of laser power to produce a stable, full-penetration weld. The focal spot size of the laser was 333-µm (200-µm fiber diameter, 250-mm focusing lens). A travel speed of 80-IPM was used. The equipment set-up and cross-section of a good weld are shown in Fig. 1. The second group of laser welds targeted partial-penetration welds (LOP). To obtain partial-penetration welds the laser power was reduced to 9-kW. All other parameters remained the same. The third group of laser welds targeted full-penetration welds that were slightly misaligned (MS) with the joint so that lack-of-fusion would results. These welds were made with the same parameters as the first series of welds, but the motion program was altered to ensure that lack-of-fusion would result.

EDDY CURRENT ARRAY TECHNIQUE AND RESULTS

The array system used for the inspection of laser joints is shown in Fig. 2. The array sensor is mechanically attached to an XY scanner. The array coils are connected to a multiplexer. The multiplexer and the XY scanner are connected to a data acquisition and

conditioning unit MS5800. A notebook computer connected to the MS5800 unit controls the entire acquisition, processing, and data storage process with MultiView software. The sensor consists of 64 coils in four rows. The first two rows are staggered with respect to the other two rows. The coils are arranged in transmit-receive pairs forming 32 axial (A-ch) and 30 transverse (T-ch) channels. This arrangement allows detection and sizing of flaws with any orientation. The array resolution along the X and Y axis on the plane is 1.25-mm. The data was acquired with resolution of 0.25-mm along the direction of probe scanning (A-ch direction). During each scan, the array was excited at 4 frequencies simultaneously: 100 kHz, 400 kHz, 800 kHz, and 1.2 MHz distributed in 16 time slots.

System Calibration and Scanning Pattern

A calibration specimen shown in Fig. 2 was designed and fabricated with six electrical discharge machining (EDM) notches for equipment calibration. Three of the notches with depth 2-, 1- and 0.5-mm were cut through the specimen width. The other three notches with different depth 2-, 1-, and 0.5-mm (similar to through-width notches) had a circular shape with a different length on the specimen surface. The specimen was made from the same material as the laser welded specimens tested in this project – austenitic stainless steel 316L.

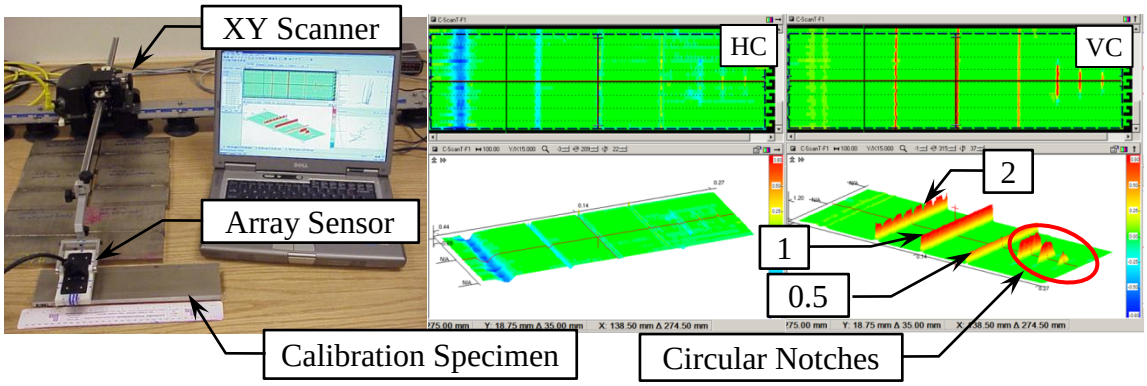

FIGURE 2. Eddy current array system with sensor mounted on XY-scanner and T-ch calibration screens at 100 kHz.

Calibration screens (T-ch) from a scan of the calibration specimen are shown in Fig. 2 as well. A C-scan and Isometric View screens present color coded signal strength for the vertical (VC) and horizontal (HC) components of the eddy current signals. All frequencies and channels were standardized to have 1 V signal VC from a through-width notch with depth of 1-mm. Because of the channels directional sensitivity, the T-ch were calibrated during a calibration specimen scan with the sensor oriented as shown in Fig. 2 with the T-ch parallel to the EDM notches. The A-ch were calibrated after rotating the array probe in the scanner holder at 90 deg and performing a calibration specimen scan so that the A-ch were parallel to the EDM notches. It is important to note that the actual depth of penetration at the lowest frequency 100 kHz was limited to approximately 1-mm as shown in Fig 2 on VC window for this type of coil configuration

Two scans longitudinal or axial (A-sc) and transverse (T-sc) as shown in Fig. 3 were performed on each surface top (Tp) and bottom (Bm) of the specimens. For field inspections, one A-sc following the weld torch will be sufficient if a specialized probe is designed for inspection of narrow laser welds with 1- to 2-mm width. The off-the-shelf sensor used in this project had spatial resolution of 1.25-mm comparable to the weld width

in direction perpendicular to weld length and required the high resolution (0.25-mm) T-sc perpendicular to the weld length.

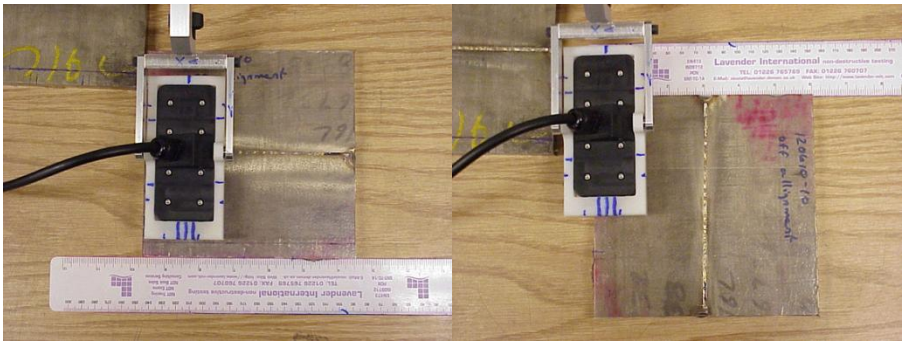

FIGURE 3. Weld Specimen A-sc (left) and T-sc (right).

The automated eddy current techniques allowed fast data acquisition of significant amount of data in short time. For example, 192 data sets (2 scans x 12 surfaces x 2 channel types x 4 frequencies) were acquired and 382 plots (VC and HC of signal) were available for analysis. The A-sc of each weld surface took up to 10 s while the T-sc took approximately 40 s to cover the surface. Most of the time during inspection was spent on changing and fixing the specimens in a position for scanning.

Welds with LOP

Comparison of top surfaces of acceptable (W1G and W6G) specimens to top surfaces of specimens with LOP on bottom surfaces (W8LOP and W9LOP) is shown in Fig. 4. Pictures of specimen top surfaces are shown in Fig. 4 scaled and vertically flipped to match the length and XY orientation on color coded eddy current C-scans. The difference between crown indications was similar and easily detectable on the A-sc T-ch scans. One reason for this difference was that the crown reinforcement (crown height) was larger on the LOP specimens. It was confirmed by other HC plots at higher frequency (e.g 1.2 MHz). Lower power was used to produce the LOP. Without dedicated metallographic analysis, it was not clear whether the weld grain and phase structure were different between the acceptable and LOP specimens.

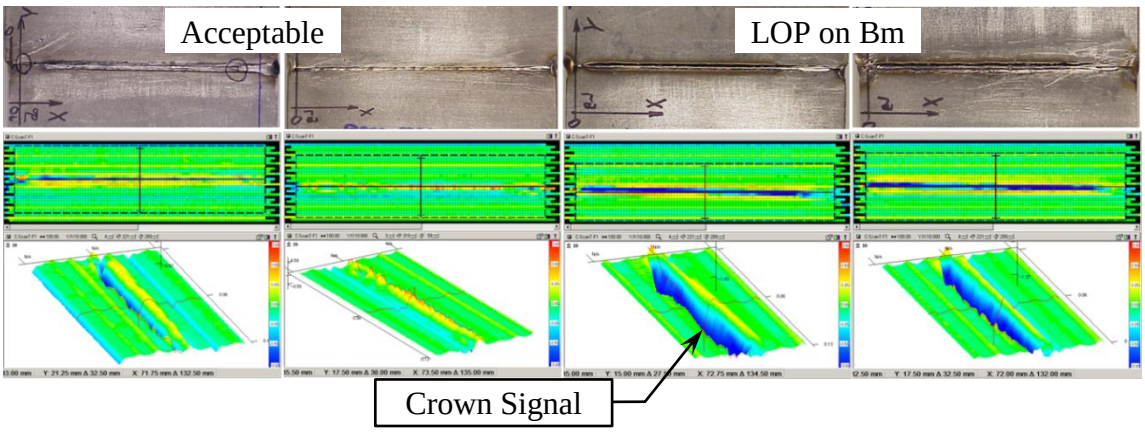

FIGURE 4. Acceptable welds (left) versus welds with LOP (right) on Bm surface. (Tp, A-sc, T-ch, 100 kHz)

Results from scanning Bm surfaces for acceptable and LOP specimens are shown in Fig. 5. The T-ch with major direction of sensitivity parallel to the weld root indicated clear distinction between acceptable and LOP root condition.

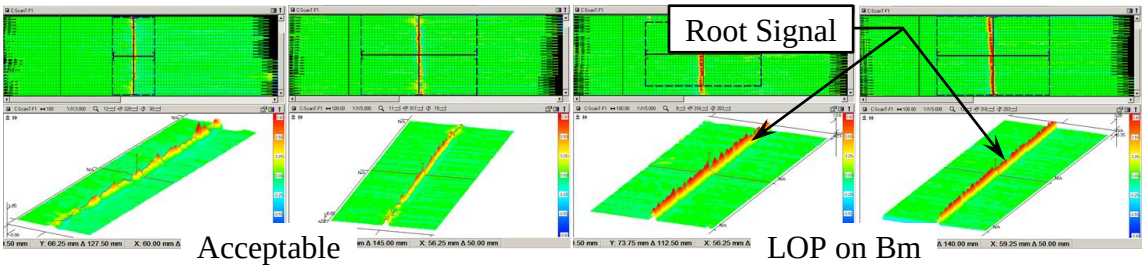

FIGURE 5. Acceptable welds (left) versus welds with LOP (right) on Bm surface. (Bm, T-sc, T-ch, 100 kHz)

Welds with Missed Seam

The missed seam at specimen start and stop ends was easily visible and detectable, especially on the HC of the channels shown in Fig. 6. A background subtraction along the direction of scanning was very effective in suppressing the weld crown surface noise and allowing better accuracy of MS length measurement. Higher magnification start and stop area pictures on each side of the W10MS eddy current plot clearly indicated the location of the MS as detected on the inspection plot. The eddy current transverse scans of W11AMS indicated that the specimen did not have MS condition and produced weld pattern similar to acceptable weld in Fig. 6.

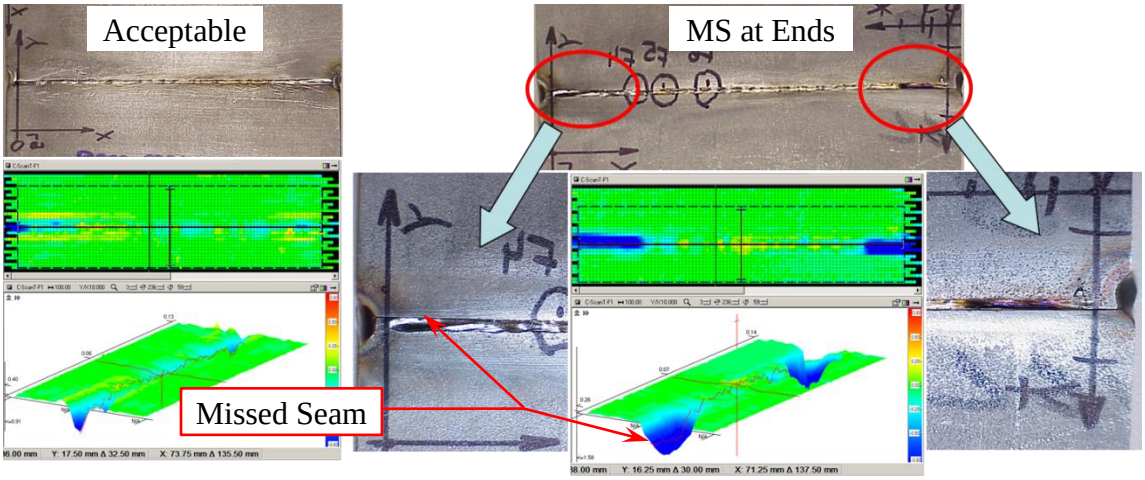

FIGURE 6. Acceptable weld (left) versus weld with MS (right). (Tp, A-sc, T-ch, 100 kHz)

The bottom surfaces of acceptable (W1G and W6G) specimens and a specimen with MS (W10MS) were also inspected. On average, the MS length at the start end of the specimen was 29.2-mm and 41.8-mm on the Tp and Bm surfaces respectively. The average length of MS at the specimen stop end on the Tp and Bm surfaces was 20-mm and 24-mm respectively. The MS length on the Bm surface was larger than the MS on the Tp surface. The difference between the MS length on the Tp and Bm surfaces was caused by the fabrication technique used to introduce the MS and the slightly decreasing weld width with the increased distance or depth from the weld crown.

Welds Surface Profile

A number of additional flaw indications were detected and recorded. The threshold for recording was set at 1 V VC which was approximately twice larger than the weld surface background. Most of the flaws produced the largest signal at the lowest frequency of 100 kHz. The largest number of flaw indications were detected on Tp and Bm surfaces of specimen W11AMS. One particular location on bottom surface of W1G produced characteristic indication shown in Fig. 7. The specimen W1G was sectioned at that location to validate the array eddy current indications.

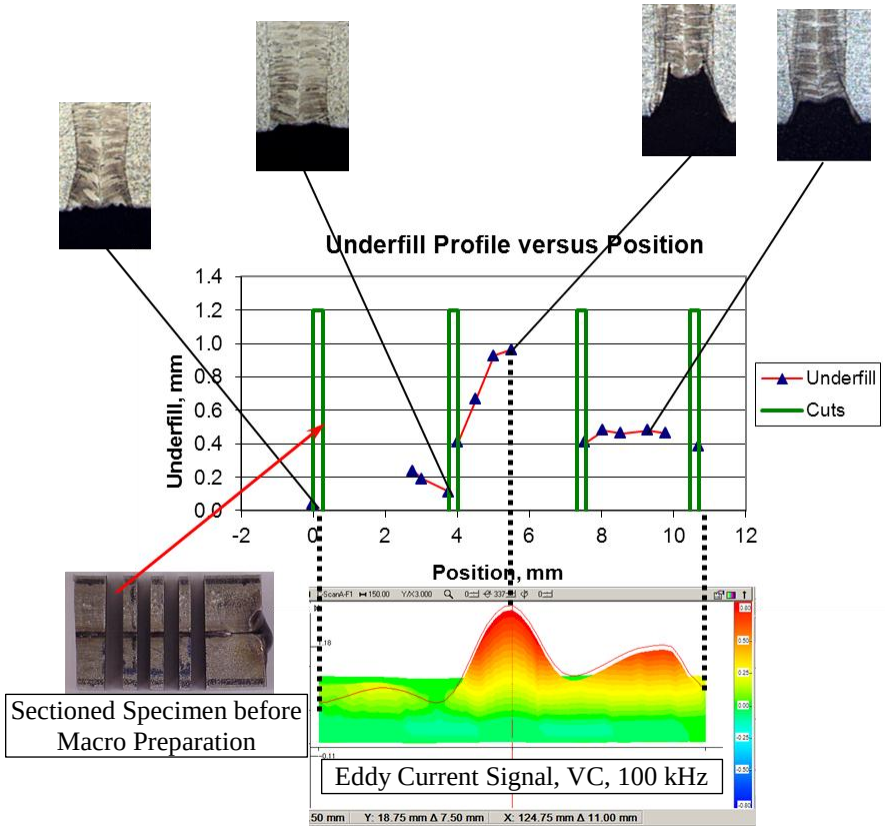

FIGURE 7. Destructive test validation of eddy current indication for underfill profiling.

A piece from the specimen W1G was extracted for further sectioning and validation of the indications. The W1G extracted piece was sectioned at four locations as shown in Fig. 7 using an EDM process. The EDM cuts had a width approximately 0.25-mm. Each of the five smaller pieces was analyzed metallographically to determine the cause of the indications. The macros were ground, polished, and etched, and images were acquired at different steps depending on the location. The analysis determined that the source of the indications was localized underfill. The underfill depth profile along with weld-root-macro images are shown in Fig. 7. The EDM cut width at each cut location was accounted for when plotting the profile. Obviously, no profile data was available for areas consumed during the EDM cutting process. The strength of the VC of the array indication, also shown in Fig. 7, matched the LOP profile. The advanced array eddy current technique demonstrated excellent capabilities to detect, image and size short (less than 2-mm) and shallow (less than 1-mm) underfill.

CONCLUSIONS

The following conclusions can be drawn from this study:

- The detection, imaging, and length sizing of typical laser weld flaws such as missed seam and LOP was demonstrated.
- The detection, imaging, length sizing, and even depth profiling of short and shallow flaws (e.g. underfill) was also demonstrated. Some of the eddy current indications were validated through destructive testing.
- The data generated with the advanced array EC techniques are easy to interpret and can be automated for fast in-line inspection and control of welding process.

ACKNOWLEDGEMENTS

This study was supported by the Department of Energy under Award Number DE-NE0000279, through the Nuclear Fabrication Consortium (NFC) managed by Edison Welding Institute (EWI).

REFERENCES

1. R. A. Matzie, "The Nuclear Renaissance – Implications on Quantitative Nondestructive Evaluations," in *Review of Progress in QNDE*, **26A**, edited by D. O. Thompson and D. E. Chimenti, AIP Conference Proceedings vol. 894, American Institute of Physics, Melville, NY (2007), pp. 3-16.
2. S. R. Doctor, "Nuclear Power Plant NDE Challenges – Past, Present and Future," in *Review of Progress in QNDE*, **26A**, edited by D. O. Thompson and D. E. Chimenti, AIP Conference Proceedings vol. 894, American Institute of Physics, Melville, NY (2007), pp. 17-31.
3. E. I. Todorov, W. C. Mohr and M. G. Lozev, "Detection and Sizing of Fatigue Cracks in Steel Welds with Advanced Eddy Current Techniques," in *Review of Progress in QNDE,* **27B**, edited by D. O. Thompson and D. E. Chimenti, AIP Conference Proceedings vol. 975, American Institute of Physics, Melville, NY (2008), pp. 1058-1065.
4. D. C. Hurley, K. H. Hedengren, P. J. Howard, W. P. Kornrumpf, G. E. Sutton and J. D. Young, "An Eddy Current Array System for Aircraft Engine Inspections," in *Review of Progress in QNDE,* **13A**, 1994, Brunswick, Maine; United States; 1-6 Aug. 1993, pp. 1111-1118.
5. M. Uesaka, T. Nakanishi, K. Miya, H. Komatsu, K. Aoki. and K. Kasai, "Micro Eddy Current Testing by Micro Magnetic Sensor Array," in *IEEE Transactions on Magnetics,* **31**, No. 1, January 1995, pp. 870-876.
6. N. Goldfine and K. Walrath, "Nondestructive Coating Characterization and Flaw Detection, Using a Conformable Meandering Winding Magnetometer (MWM)," in *Fifth EPRI Steam Turbine/Generator Workshop*, Lake Buena Vista, Florida, August 1, 1997.
7. C. Gilles-Pascaud, J. M. Decitre, F. Vacher, C. Fermon, M. Pannetier and G. Cattiaux, "Eddy Current Flexible Probes for Complex Geometries," in *Review of Progress in QNDE,* **25A**, edited by D. O. Thompson and D. E. Chimenti, AIP Conference Proceedings vol. 820, American Institute of Physics, Melville, NY (2006), pp. 399-406.

Paper published in the QNDE 2012 Proceedings, by the American Institute of Physics, www.aip.org